Finite-temperature study of itinerant ferromagnetism in Fe, Co, and Ni

N. M. Rosengaard and Börje Johansson
Condensed Matter Theory Group, Physics Department, Uppsala University, S-75121 Uppsala, Sweden
(Received 15 January 1997)

We propose a simple model for itinerant magnetism in the ferromagnetic transition metals. The model incorporates both the energy of moment formation, and the energy of moment ordering. The parameters of the model are determined from first-principles density-functional calculations for the ferromagnetic state and a number of spin spiral states. The simplicity of the magnetic energy functional allows extensive Monte Carlo simulations to be performed. Results for the finite-temperature magnetic properties of body-centered-cubic Fe, and face-centered-cubic Co and Ni are presented. [S0163-1829(97)00722-4]

I. INTRODUCTION

In recent years, significant progress has been made in the description of magnetic ordering within theories of itinerant magnetism.[1–13] This has been achieved through the extension of band methods to describe noncollinear spin structures within the density functional scheme. The formalism has also been applied to the study of magnetic excitations, and finite-temperature properties of ferromagnets. You *et al.*[1] calculated exchange constants of bcc Fe from selected magnetic configurations, and estimated the Curie temperature by means of a Heisenberg Hamiltonian and the mean-field approximation. Oguchi *et al.*[2] used the Korringa-Kohn-Rostoker multiple-scattering technique in the coherent potential approximation (KKR-CPA), and the disordered local moment (DLM) model to study bcc Fe at finite temperature. Similarly, Pindor *et al.*[3] combined the KKR-CPA with the DLM to study the magnetic $3d$ transition metals, Cr, Fe, Co, and Ni. Liechtenstein *et al.*[4] used the KKR formalism in the atomic-spheres approximation (ASA) to calculate exchange interactions for Fe, Ni, and Ni-Pd alloys. Luchini and Heine[5] studied short-range order, and obtained exchange interactions for bcc Fe from a large number of magnetic configurations. Staunton and Györffy[6] calculated paramagnetic susceptibilities, and Curie temperatures of Fe and Ni using an improved version of the DLM that included some short-range order effects by Onsager cavity fields. The paramagnetic susceptibilities obtained by Staunton and Györffy obey a Curie-Weiss law, as observed experimentally, but the Curie-Weiss constants were underestimated. They determined a Curie temperature (T_C) of bcc Fe in close agreement with the observed T_C, and found a somewhat underestimated value of T_C for fcc Ni. In a recent work, Uhl and Kübler[7] studied the finite-temperature properties of the ferromagnetic transition metals bcc Fe, fcc and hcp Co, and fcc Ni using a model Hamiltonian in conjunction with mean-field spin-fluctuation theory to calculate the free energy. Similar to Staunton and Györffy, they find a Curie temperature of bcc Fe which is in close agreement with the observed Curie temperature while the Curie temperatures of fcc Co and fcc Ni are underestimated. Uhl and Kübler also note that their calculated Curie-Weiss constants are underestimated by a factor ~ 2. Another very recent development, is the formulation of Antropov *et al.*[8,9] of spin dynamics within the density-functional theory. This approach eliminates the need of an assumed form of the magnetic Hamiltonian, at some cost of simplicity.

Prior to the use of density-functional formalism in the local-spin-density approximation, a description based on noncollinear local magnetic moments was adopted by several workers, in particular the work of Moriya,[14] Edwards,[15] Hubbard,[16] and Hasegawa,[17] as well as the work of Korenman and co-workers[18] inspired much of the later first-principles work on magnetic excitations, and finite-temperature properties of ferromagnets.

Simultaneously with the first-principles developments, there have been numerous studies of the statistical mechanics of model Hamiltonians known to reproduce selected magnetic properties of real magnets. It is the purpose of this paper to bridge the gap between these parallel developments by formulating a more realistic model Hamiltonian for the magnetic interactions based on results of first-principles calculations on a set of magnetic structures. The magnetic energy functional which is used in the study of Uhl and Kübler[7] is closely related to the one considered in the present study, and the parameters are obtained from the same type of magnetic structures, i.e., spin spirals. Our final expression for the magnetic energy differs slightly from theirs due to our assumption of local interatomic exchange interactions which lead directly to a real-space expression and an intrasite term rather than an expression in terms of reciprocal-space fluctuations from the ferromagnetic state, as was used by Uhl and Kübler.

The paper is organized as follows. In Sec. II, we describe the model that we use to calculate the energy of a magnetic configuration. We also describe how the model parameters are obtained from first-principles calculations within the local-spin-density approximation. In Sec. III, we present results for the low-temperature magnetic properties obtained directly from self-consistent calculations. In Sec. IV, we describe the results obtained from Monte Carlo simulations at finite temperature using our model magnetic energy functional. Section V contains some concluding remarks.

II. MODEL OF AN ITINERANT MAGNET

Below we will first present the magnetic energy functional which we have applied to describe the itinerant ferro-

magnets, Fe, Co, and Ni. Subsequently, we describe the calculation of model parameters. We will briefly outline the main ingredients that enter into the construction of the magnetic energy functional. The model is based on a coarse-grained description of the magnetic state expressed by the set of local magnetic moments $\{\overline{m_i}\}$ which is used as the basic variable in the representation of the magnetic state. It is the size and relative direction of the local exchange splittings that determine the interatomic exchange. This in turn brings us to represent the interatomic exchange interaction as an expansion in powers of the local moments, and cosine to their relative angle. Hence, the interatomic exchange is described using a generalization of the Heisenberg Hamiltonian that also incorporates the dependence on the size of the local magnetic moments. By also including an on-site exchange term, we describe in addition the energy of moment formation. In this sense, the present magnetic energy functional provides a unified description of the energetics of moment formation, as well as the energetics of moment ordering.

A. The magnetic energy functional

We now present the model which we will use to describe the magnetic energy of an itinerant magnet. As a result of the dominant *d*-orbital contribution to the magnetic moment, local atomic moments are well-defined variables within the context of a density-functional description of magnetic properties of transition metals. A description based on local moments has been extensively applied to the study of itinerant magnetism from first-principles.[1–9] In order to give a reasonably complete description of itinerant magnetism at finite temperature, we need a model that describes simultaneously the energetics of the formation of the local magnetic moment, and the magnetic ordering of the local moments.

As a starting point for the description of the moment formation energy, we use the Stoner-Wohlfarth model for the stability of the ferromagnetic state. In this model, the magnetic energy of the ferromagnetic state of moment M is given by a Ginzburg-Landau like energy expansion in the magnetization

$$E^{\mathrm{FM}}=E^{\mathrm{PM}}+\frac{1}{2}AM^2+\frac{1}{4}BM^4, \tag{1}$$

where the coefficients in the expansion are derived from the strength of the exchange interactions, and include both intra- and interatomic contributions. As it stands Eq. (1) does not include the effect of fluctuations in the moment and it also neglects the vector nature of the moment. The expression above may be generalized in this respect as, for example, was done by Mohn and Wohlfarth in their study of Curie temperatures of ferromagnetic metals and compounds.[18] The Stoner-Wohlfarth representation of the magnetic energy describes the stability of the ferromagnetic state of moment M. While the Ginzburg-Landau expansion is only valid in the vicinity of the transition from the paramagnetic to the ferromagnetic state where the moment is small, it is however possible to describe the energy of formation of the constrained ferromagnetic state of magnetization M, as an expansion in even powers of the magnetization:

$$E^{\mathrm{FM}}=E^{\mathrm{PM}}+\sum_{k=1}^{n} A_k^{\mathrm{FM}}M^{2k}. \tag{2}$$

In a first-principles approach, the coefficients in the expansion, may be obtained from so-called fixed spin moment (FSM) calculations for the constrained ferromagnetic state. This scheme was introduced by Moruzzi and co-workers.[20] For Fe, Co, and Ni, we find that typically 5–7 coefficients give an excellent least-squares fit to the calculated ferromagnetic FSM states in a range extending from the nonmagnetic state to states of moments well beyond the equilibrium ferromagnetic moment. While this approach gives an excellent description of the constrained ferromagnetic states, no distinction is made between on-site, and interatomic exchange interactions. However, in a model for arbitrary magnetic configurations, we have to introduce such a division.

To obtain a model that incorporates also the energy of magnetic ordering, it is necessary to model the interatomic exchange explicitly. This is done in the classical Heisenberg model of ferromagnetism. Atomic magnetic moments of fixed size interact via the interatomic exchange field. The energy of magnetic ordering E^{MO} becomes

$$E^{\mathrm{MO}}=-\frac{1}{2}\sum_{i\neq j} J_{ij}\overline{e_i}\cdot\overline{e_j}, \tag{3}$$

where $\overline{e_i}$ is the unit vector parallel to the local moment at site i, and J_{ij} is the exchange energy between local moments at site i and j, respectively. In the context of density-functional formalism, Liechtenstein *et al.*[4] showed that the energy change for incremental deviations from the ferromagnetic state is described by the Heisenberg Hamiltonian. They used Andersen's force theorem[21] to derive the energy change due to a rotation of the moment at the central site in a ferromagnet through an angle θ, i.e.,

$$\Delta E_0(\theta)=\frac{1}{\pi}\mathrm{Im}\int^{\epsilon_f} d\epsilon\,\mathrm{Tr}_L\ln\Bigg[1+\frac{1}{2}(1-\cos\theta)\times\sum_{j\neq 0}\Delta P_0 g_{0j}^{\uparrow}\Delta P_j g_{j0}^{\downarrow}\Bigg], \tag{4}$$

where we have adopted Andersen's linear muffin-tin-orbital (LMTO) formalism.[22] In Eq. (4) ΔP is the potential function difference between the two spin channels and g_{ij} is the ferromagnetic KKR-ASA Green's function connecting sites i and j. A similar expression was obtained by Oguchi *et al.*[13] for the interaction of two moments embedded in a CPA medium of randomly oriented moments. In the limit of small θ, one recovers the energy dependence of the Heisenberg Hamiltonian.

A Taylor expansion of the logarithm in Eq. (4) gives a power series in $\cos\theta$, and we therefore anticipate that a more complete representation of the ordering energy of an arbitrary magnetic configuration can be obtained by including also pair interactions, and if required multisite interactions, which are higher powers of the cosine of the relative angle. In such an expansion, the first term is the Heisenberg term (J_{ij}), while the second (K_{ij}), and third order (L_{ij}) pair interactions are denoted as the biquadratic, and the bicubic term, respectively.

Further, by means of the expression of Liechtenstein *et al.*, we can trace the dependence of the interatomic exchange on the size of the local magnetic moments through the potential function difference ΔP between the minority- and majority-spin channel. This difference is essentially the exchange splitting of the one-electron potential. In a simplified Stoner model, it is related to the size of the magnetic moment, i.e., $\Delta P_i \simeq m_i I$, where the local spin-up and spin-down density of states are considered rigidly shifted by the exchange splitting, and I is the Stoner parameter averaged over the one-electron states crossing the Fermi surface.[23] As a result, for small deviations the magnetic ordering energy depends linearly on the size of the local moments m_i, i.e., $E^{\mathrm{MO}} \propto -\Sigma_{\langle ij \rangle} J_{ij} \langle m_{ij} \rangle^2$ where $\langle m_{ij} \rangle$ is an appropriate average, to be specified below, of the size of the local moments m_i, and m_j that constitute the pair $\langle ij \rangle$. To describe a general magnetic configuration, we therefore include the dependence of the interatomic exchange on the size of the local magnetic moment. This dependence is included by expressing the interatomic exchange constants J_{ij}, K_{ij}, etc. of the Heisenberg term and the higher-order pair terms, in a power series in the size of the local moments.

Following our generalization of the Stoner-Wohlfarth expression for the constrained ferromagnetic states to cover the whole range of local moments, we analogously arrive at the following expansion which we use to represent the interatomic exchange energy:

$$E^I = -\frac{1}{2}\sum_{i \neq j} J_{ij} \overline{e_i} \cdot \overline{e_j} - \frac{1}{2}\sum_{i \neq j} K_{ij} (\overline{e_i} \cdot \overline{e_j})^2, \tag{5}$$

where

$$J_{ij} = \sum_{k=1}^{n} J_{ij}^k \langle m_{ij} \rangle^{2k}, \quad K_{ij} = \sum_{k=1}^{n} K_{ij}^k \langle m_{ij} \rangle^{2k}, \tag{6}$$

In these equations, J_{ij}^k and K_{ij}^k are the coefficients in the expansion of the Heisenberg term and the biquadratic term, respectively. Other terms such as the bicubic pair L_{ij} and multi-site interactions of the type $(\overline{e_i} \cdot \overline{e_j})(\overline{e_i} \cdot \overline{e_k})$ can be treated similarly if they are required for an accurate description of the magnetic energy. In the above expression, we use for the local moment, $\langle m_{ij} \rangle$ the simple average of the local moments m_i and m_j of site i, and j respectively.

To determine the dependence of the exchange constants on varying the local moments independently, we performed self-consistent calculations of longitudinal spin fluctuations from the ferromagnetic state and found for Fe, Co, and Ni that using the simple average of the local moments gave an excellent description of the energy of these fluctuations. The choice of $\langle m_{ij} \rangle$ as the simple average results in a nonzero interatomic exchange interaction if one local moment tends to zero while the other moment remains constant. The error that this induces, is insignificant since, for all finite temperatures, the local moments will be fluctuating around a value close to the zero-temperature magnetization. The actual calculation of the interatomic exchange constants (J_{ij}^k, K_{ij}^k, etc.) is performed by application of the FSM technique to the spin spiral states and a subsequent fitting of the total energy of the spin spiral states relative to the energy of the ferromagnetic state with the same local moment.

Having accounted for the interatomic exchange, we now proceed to derive the on-site exchange term from the FSM calculations for constrained ferromagnetic states. Hence, we represent the on-site exchange by an expansion similar to the one describing the total energy of the FSM state, i.e.,

$$E^{\mathrm{on}} = \sum_i \sum_{k=1}^{n} A_k^{\mathrm{on}} m_i^{2k},$$

$$A_k^{\mathrm{on}} = A_k^{\mathrm{FM}} + \frac{1}{2}\sum_j (J_{0j}^k + K_{0j}^k), \tag{7}$$

where j labels the sites in the neighbor shells of the central site 0. Finally, to get the total magnetic energy of an arbitrary magnetic configuration, we add the on-site contribution E^{on} of Eq. (7) to the interatomic exchange E^I given in Eq. (5).

An important consequence of our chosen total-energy functional, is that it describes the reduction of the local magnetic moment as the local exchange field decreases due to the disorder in the orientational degrees of freedom. It should be realized that the on-site term can be viewed as the energy of embedding a single magnetic atom into the nonmagnetic state of the metal. For an itinerant magnet, the on-site term is therefore not only an atomic contribution but depends strongly on the response of the ligand states to the impurity moment. To get a practical scheme, we have to estimate the convergence of the expansion Eq. (5) for the interatomic exchange. In the actual calculations, we always neglected multisite interactions, as well as powers of $\cos\theta$ beyond the bicubic term in the pair interactions. The pair interactions were furthermore restricted to either the nearest or next-nearest shell of neighbors. Even so, we reproduce very accurately the energetics of the set of spin spirals for which first-principles calculations were performed. For the power-series expansion given in Eq. (6) of the dependence of the exchange constants on the local magnetic moments, we used $\sim$ 3–4 terms.

B. Computational details

In this section, we give the computational details of the first-principles calculations for Fe(bcc), Co(fcc), and Ni(fcc), that are used to derive the parameters of the model which was described above. We have applied the density-functional formalism in the local-spin-density approximation (LSDA) to calculate the total energy of a set of magnetic structures for the $3d$ ferromagnets Fe, Co, and Ni. We employed the parametrization of Vosko-Wilk-Nusair[24] for the exchange and correlation contributions in the LSD approximation. The first set of calculations consisted in the determination of the energy versus magnetic moment curves of the ferromagnetic state. For each of the metals, we have fixed the volume at the calculated equilibrium volume. The second set of calculations were total-energy calculations of planar spin spiral states along high-symmetry directions. For the bcc structure, we chose the [011] and the [001] directions. For the fcc structure, we used the [111] and the [001] directions. Calculations were performed for the spin spiral wave vectors $|\overline{q}| = \frac{1}{16}, \frac{1}{8}, \frac{1}{4}$, and $\frac{1}{2}$ in units of the longest reciprocal-lattice vector in each direction. The spin spiral states were calcu-

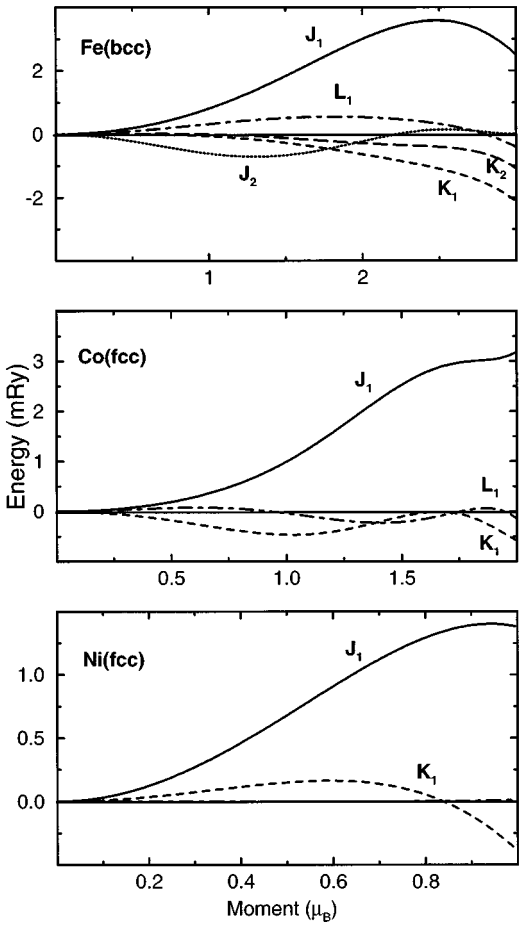

FIG. 1. The interatomic exchange constants for bcc Fe (top), fcc Co (middle), and fcc Ni (bottom). The Heisenberg term (J_i), biquadratic term (K_i), and bicubic term (L_i) for ith nearest neighbors are shown as a function of the local magnetic moment.

lated using the LMTO-ASA method[25,26] in the tight-binding representation of Andersen and Jepsen.[27] The implementation of noncollinearity follows the scheme described by Uhl *et al.*, see Ref. 12, and references therein. We also included the combined correction term to the One-electron Hamiltonian. This was implemented as described by Antropov *et al.*[9] For the spin spiral states, as well as for the ferromagnetic states, we applied the FSM technique to study the dependence of the interatomic exchange on the size of the local moments. We used the FSM technique in an implementation similar to the one of Uhl *et al.*[12] In this implementation, an auxiliary local magnetic field is introduced. This field is determined by the requirement of a fixed local magnetic moment. The total-energy differences between the spin spiral states and the ferromagnetic state with the same local magnetic moments are used to derive the interatomic exchange constants by least-squares fitting to the model expression for the interatomic exchange. Figure 1 shows the resulting exchange parameters for bcc Fe, fcc Co, and fcc Ni as a function of the local magnetic moment. For all three metals, the nearest-neighbor Heisenberg term, denoted J_1, is the dominating interaction. We stress the fact that the exchange interactions are renormalized ones, and that the direct calculation of the exchange parameters as suggested by Liechtenstein *et al.*[4] may very well result in long oscillatory interactions.

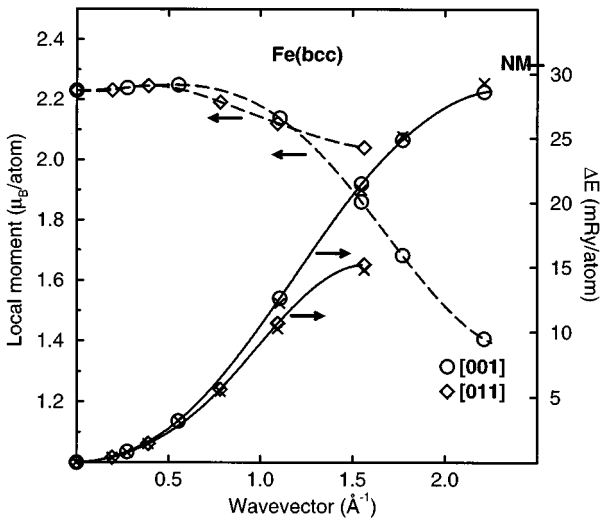

FIG. 2. Calculated total energies (full lines) of planar spin spiral states in bcc Fe relative to the energy of the FM state. Also shown (dashed lines), are the equilibrium local moments of the spiral states. All lines are fit to the calculated values which are shown by symbols. Diamonds represent calculations in the [011] direction. Circles are results for the [001] direction. Crosses indicate spiral energies calculated from the model expression for the interatomic exchange. NM indicates the energy of nonmagnetic bcc Fe relative to the energy of FM bcc Fe.

What is obtained by the fit is an adequate description of the spin spiral states. The accuracy of the fit in reproducing the spiral energies can be estimated by inspection of Figs. 2, 3, and 4 for, respectively, bcc Fe, fcc Co, and fcc Ni. It should be noted that the spin spirals whose energy is shown in the figures, are the planar spin spirals which result when the magnetic moment is allowed to relax to its preferred value whereas we have applied the spin spirals with constrained local moments to calculate the exchange constants. We

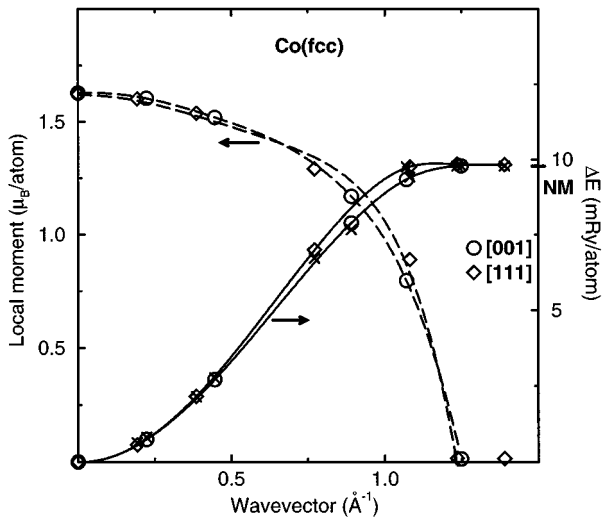

FIG. 3. Planar spin spirals in fcc Co. Notation as in Fig. 2. NM indicates the energy of nonmagnetic fcc Co relative to that of FM fcc Co. Note that zone boundaries are not shown. The [001] zone boundary is at 1.78 $Å^{-1}$. The [111] zone boundary is at 1.55 $Å^{-1}$.

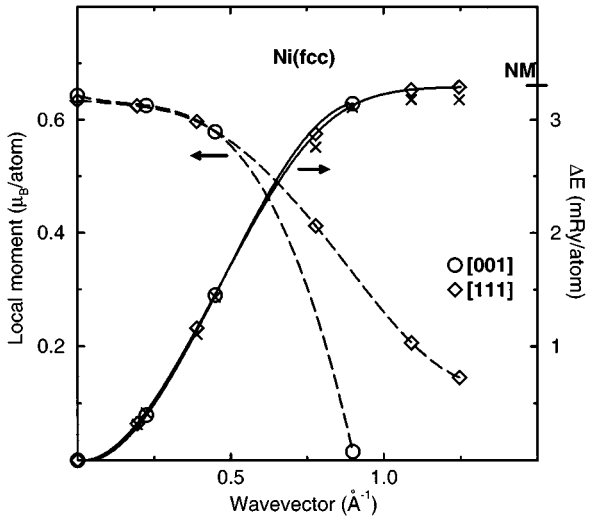

FIG. 4. Planar spin spirals in fcc Ni. Notation as in Fig. 3. The zone boundaries are not shown. The [001] zone boundary is at 1.80 Å^{-1}. The [111] zone boundary is at 1.56 Å^{-1}.

tested the sensitivity of the exchange parameters to the size of the set of spin spiral states used in the fitting procedure, and found only insignificant changes in the calculated parameters. We also note that ultimately we will use the exchange interactions to study the finite-temperature magnetic properties in Monte Carlo simulations. For Fe, we tested the effect of using a smaller set of interactions at a simulation temperature close to the critical temperature. In this case, the effect of changing the set of interactions was of the order of the statistical errors. We take this as an indication that the derived set of exchange parameters are reasonably complete within the description used for the interatomic exchange. Additionally, we show below that our model prediction of energy and local moment stability in the disordered local moment configuration compares favorably to the results obtained from KKR-CPA calculations. However, the possibility exists that a larger set of more general magnetic configurations will show that further interactions such as interactions of longer range or multisite interactions are in fact important.

III. SCF CALCULATIONS

In what follows, we first present the self-consistent LMTO calculations of zero-temperature magnetic properties of the ferromagnetic transition metals Fe, Co, and Ni. Subsequently, we discuss the parameters of the model, and their implications for the picture of the itinerant magnetism of the transition metals.

A. Zero-temperature magnetic properties

Table I contains some magnetic ground-state properties. Shown in the table are both the values obtained in the present study, and where available the experimental values. As is well known, the calculated equilibrium lattice constants depend to some extend on the type of exchange-correlation potential one employs. In the local-spin-density approximation the lattice constants for all three metals are underestimated. However, the errors are at the 1% level. The 0 K magnetic moments are also given in Table I. We notice that since the observed moments include an orbital contribution of about $0.1\mu_B$, the calculated spin magnetic moments are slighty overestimated in the cases of Ni and Fe.

TABLE I. Comparison between calculated, and experimental ground-state properties, where a_{eq} is the equilibrium lattice constants, M is the zero-temperature magnetization, D is the spin-wave stiffness constant. The experimental spin-wave stiffness constants are extrapolations to zero temperature, except for Co, where the room-temperature value for the hexagonal close-packed structure is given. All experimental numbers are labeled Expt.

System	a_{eq} (Å)		M (μ_B/atom)		D (meV Å^2)	
	Calc.	Expt.	Calc.	Expt.	Calc.	Expt.
Fe bcc	2.84	2.87	2.23	2.25[a]	247	314[c]
Co fcc	3.52	3.55	1.63	1.72[b]	502	510[d]
Ni fcc	3.49	3.52	0.64	0.62[a]	739	550[e]

[a]Reference 28.
[b]Reference 29.
[c]Reference 30.
[d]Reference 31.
[e]Reference 32.

The spin-wave stiffness constant D that relates the spin-wave frequency ω to the wave vector in the long-wavelength limit as $\omega = Dq^2$ may be calculated from the energy of spin spiral excitations. The relation between the spin-wave stiffness and the energy cost of forming a spin spiral can be derived by noting that the total magnetization loss caused by a spin-wave excitation is $2\mu_B$, while the magnetization loss per site $\Delta M = M_{eq}(1-\cos\theta)$ tends to zero. Hence the energy of a spin-wave excitation is

$$\omega(\overline{q}) = 2\mu_B \left.\frac{\Delta E^s(\overline{q},\theta)}{\Delta M}\right|_{\theta=0} = \frac{4\mu_B}{M_{eq}} \Delta E^{ps}(\overline{q}), \tag{8}$$

where $\Delta E^s(\overline{q},\theta)$ is the energy of a spin spiral of wave vector $\overline{q}$, and angle θ to the magnetization direction. M_{eq} is the equilibrium magnetic moment, and $\Delta E^{ps}(\overline{q})$ is the energy of a planar spin spiral. To derive this relation, we have exploited that the energy of a spin spiral is related to the planar spin spiral of the same wave vector by $\Delta E^s(\overline{q},\theta) \simeq \sin^2\theta \Delta E^{ps}(\overline{q})$. We have established this relation, which was also noted by Uhl and Kübler,[7] empirically by performing self-consistent calculations of nonplanar spin spiral energies. The relation is exact for a Heisenberg Hamiltonian, and holds to a good approximation also for the magnetic energy functional used in this work. Hence, we can calculate the spin-wave stiffness constants from

$$D = \frac{2\mu_B}{M_{eq}} \left.\frac{d^2 E^{ps}(\overline{q})}{d\overline{q}^2}\right|_{q=0}$$

$$= \frac{1}{3M_{eq}} \sum_R R^2 (J_{0R} + 2K_{0R} + 3L_{0R}), \tag{9}$$

where we have exploited the cubic symmetry, and our parametrization of the magnetic energy to obtain the second equality. In the above expression, J_{0R}, K_{0R}, and L_{0R} denote the bilinear, the biquadratic, and the bicubic exchange con-

stants, respectively. The exchange constants are those of the ferromagnetic equilibrium magnetic moment.

As Table I shows, the calculated spin-wave stiffness constant of fcc Co compare well with the experimental value while the calculated value for bcc Fe is somewhat underestimated, and the value for fcc Ni is overestimated. Since the spin-wave stiffness constant is related to the long-wavelength limit of the spin spiral excitations, its value is independent of the inclusion of biquadratic, and bicubic terms. This is not apparent from Eq. (9). However, fitting the spin spiral energies to a Hamiltonian of the pure Heisenberg form results, within a few percent, in the same spin-wave stiffness constant. We therefore conclude that the inclusion of the higher-order terms are mainly important for the description of the short-wavelength spin spirals.

Figure 2 shows, for bcc Fe, the self-consistently calculated total energy of planar spin spiral states along the [001] and [011] directions relative to the energy of the equilibrium ferromagnetic state. Also shown are the calculated equilibrium local moments. The itinerant nature of the exchange interaction gives rise to the strong dependence of the local moment on the reduction of the exchange field as the spiral vector approaches the antiferromagnetic spin alignment at the zone boundary. The effect is most pronounced in the [001] direction, in which the antiferromagnetic structure results in all nearest-neighbor spins being antiparallel. At the zone boundary in the [011] direction, only four of the eight spins in the nearest-neighbor shell are antiparallel. Hence, for the [011] direction the reduction of the local moment for increasing spiral vector is moderate. Since the energy difference of the ferromagnetic to the nonmagnetic state is 31 mRy/atom at fixed volume, we note that the Fe magnetic moment is stabilized by less than 3 mRy/atom at the [001] zone boundary. For both fcc Co and fcc Ni, the dependence of the local magnetic moment on the spin spiral vector is more pronounced than in the case of bcc Fe. As Figs. 3 and 4 show, the planar spiral states of large wave vectors are unstable relative to the nonmagnetic state. For Ni in the [001] direction, planar spiral states are only found for spiral vectors $q \sim (1/2)q_{\max}$. In the [111] direction planar spiral states are found at somewhat larger vectors, the energy of these states is, however, only marginally smaller than the energy of the nonmagnetic state whose energy relative to the energy of the FM state is indicated in the figure. For all three systems, in a region close to the spiral vector $\overline{q}=0$, the planar spirals have an isotropic energy spectrum, as they must. For Ni, we also performed calculations for the [011] direction which has the zone boundary at 2.54 Å^{-1}. In this direction, we find that the isotropic region is somewhat narrower extending only to $q \sim 0.3$ Å^{-1}. Already from the difference in the stability of the spin spiral excitations, we can conclude that fcc Co and fcc Ni show stronger effects of itinerancy than bcc Fe. This conclusion will be substantiated when we discuss the implications of our model magnetic energy functional.

B. The energetics of the model

Figure 5 shows the total energy of the constrained ferromagnetic states of, respectively, bcc Fe, fcc Co, and fcc Ni, as a function of the magnetic moment. Also shown are the

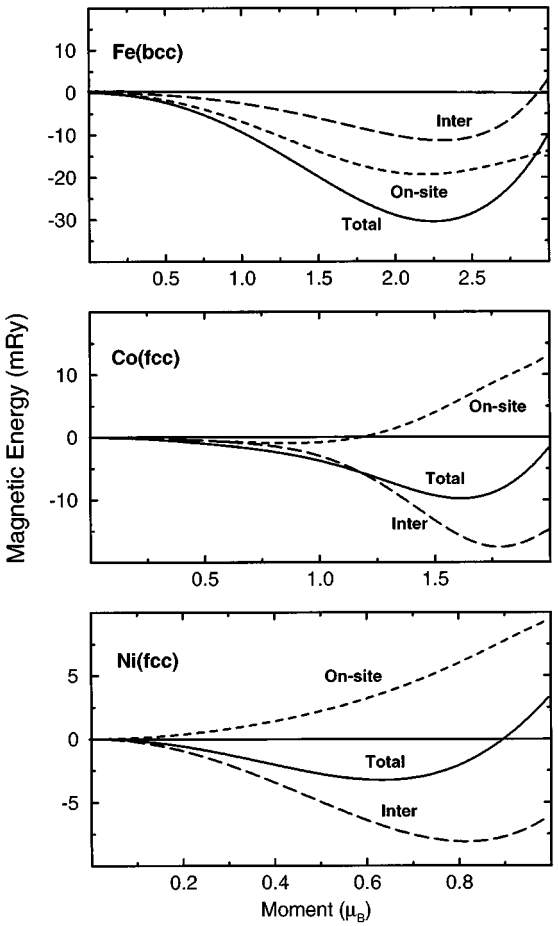

FIG. 5. The magnetic energy of, and the model contributions to, the constrained FM states of respectively bcc Fe, fcc Co, and fcc Ni. The full line (total) denotes the total magnetic energy of the constrained FM state, as calculated in FSM calculations. The short dashed line (on-site), denotes the on-site contribution to the moment formation energy, while the long dashed line (inter) is the interatomic exchange contribution.

on-site and interatomic model contributions to the total magnetic energy. One important observation that can be made based on the model contributions to the energy of the ferromagnetic state, is that the stability of the local magnetic moment for bcc Fe, due to its large on-site exchange contribution, is relatively independent of the ordering of the local moments. In contrast, the stability of the local moments of Co, and in particular of Ni depend strongly on the ordering of the local moments. Based only on the energetics, this suggests that the local moment picture works well for bcc Fe, and less so for fcc Co and Ni. These conclusions are similar to the ones reached by Pindor *et al.*[3] who applied the so-called disordered local moment (DLM) model to the description of the random, high-temperature magnetic state of bcc Fe and fcc Ni. As noted earlier, the on-site term represents the energy of an ''impurity'' moment embedded into the nonmagnetic state of the metal. However, in the DLM state consisting of randomly oriented local magnetic moments of the same size, on the average, only the biquadratic part of the interatomic exchange contributes to the stability of the local magnetic moment. The magnetic energy of the DLM state of local moments of size m_{loc} becomes

$$E^{\mathrm{DLM}}(m_{\mathrm{loc}}) = E^{\mathrm{on}}(m_{\mathrm{loc}}) - \frac{1}{6}\sum_j K_{0j}(m_{\mathrm{loc}}). \qquad (10)$$

It may be realized from Fig. 1 that the biquadratic term, i.e., the last term in Eq. (10) is small in all cases so that to a good approximation, the on-site contribution gives a measure of the stability of the local moment in the random configuration. Hence bcc Fe has a stable magnetic moment close to the ferromagnetic equilibrium moment in the configuration of randomly oriented local moments. Similarly, fcc Co has a local moment $m_{\mathrm{loc}} \sim 0.9\mu_B$ in the random configuration, while fcc Ni does not have a stable local moment at all in the DLM configuration. These results are in good agreement with the DLM calculations performed by Pindor *et al.*[3]

It is also interesting to note that despite the stable DLM solution of fcc Co, we do not find the antiferromagnetic (AFM) structure along the [111] direction to be stable, although in both configurations, the average nearest-neighbor correlation $\langle \overline{e_i} \cdot \overline{e_j} \rangle = 0$. It is the biquadratic term which destabilizes the AFM structure in fcc Co. This may be realized from Fig. 1 which shows that the biquadratic term will contribute 0.75 mRy/atom to the destabilization of the DLM state for a local moment of size $m_{\mathrm{loc}} = 0.9\mu_B$. This is slightly less than the on-site gain in energy ~ 0.9 mRy/atom. For the [111]-AFM structure, however, the biquadratic term will contribute 2.25 mRy/atom sufficient to destabilize this structure. These simple considerations clearly shows that the magnetic energy functional used in this work is capable of describing even the small energy differences responsible for the stability of the DLM state, even though this state represents the opposite limit of the coherent spin spiral states that we use to derive the magnetic energy functional. However, the Monte Carlo simulations will show that at finite temperatures, the entropy of spin fluctuations stabilizes the DLM states of Fe, Co, and Ni.

IV. FINITE-TEMPERATURE RESULTS

In this section, we describe the results of Monte Carlo (MC) simulations for the $3d$ ferromagnets Fe, Co, and Ni. We have applied the magnetic energy functional outlined in the previous section, and the standard Metropolis algorithm[32] to study the finite-temperature properties. We performed runs for system sizes ranging from ~ 700 to ~ 2700 sites applying periodic boundary conditions. One MC step consisted of a single local moment update in which we choose at random a different direction and size of the local moment. In this way, we propagate through the full configurational space $\{\overline{m_i}\}$, and consequently we describe the effect of fluctuations in both the orientational degrees of freedom, and the size of the local moments. From these calculations, we extrapolate to the thermodynamic limit using standard finite-size scaling theory. The MC simulations result, after appropriate scaling to infinite system size, in a magnetization curve, and a Curie temperature T_C. Alternatively, the Curie temperature can be estimated from the peak in the magnetic susceptibility. While the actual value of the magnetic susceptibility depends on the number of sites, the peak position of this quantity as a function of temperature did not show any size dependence. Finite-size scaling also provides information on the static critical exponents of the magnetization. However, in the present study we found it to be too expensive computationally to reliably estimate the critical exponents. The finite-size scaling was, however, sensitive to the choice of Curie temperature, and the best fit of the universal scaling function was obtained for a Curie temperature in the vicinity of the Curie temperature derived from the susceptibility. From the MC simulations, one may study the temperature dependence of the local magnetic moment, as well as the magnetic short-range order. The latter quantities only depend weakly on the number of sites.[34]

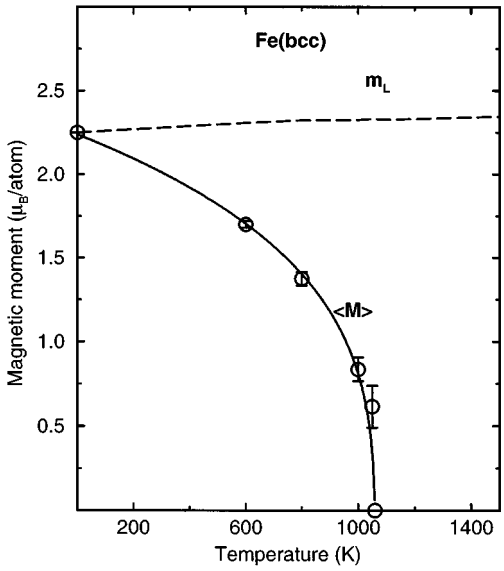

FIG. 6. The magnetization (full line), and the local magnetic moment (dashed line) of bcc Fe as a function of temperature. The results are obtained from Monte Carlo calculations, and subsequent finite-size extrapolations.

A. The magnetization curve

In Fig. 6, we show the magnetization and the local moment of bcc Fe as a function of temperature, obtained from simulations, and for the magnetization after finite-size scaling. In Figs. 7 and 8, we show similar results for fcc Co and fcc Ni. We note that the error bars on the magnetizations indicate only the statistical error from individual MC runs, and they do not include the error arising from the extrapolation procedure. The statistical error of the local moment is in all cases $< 0.01\mu_B$. The effect of changing the number of sites was even smaller for the local magnetic moments. It is seen that in all three cases the magnetization is reduced from its zero-temperature value already at moderate temperatures relative to the Curie temperature. If we compare the magnetization at a temperature $T = \frac{1}{2}T_C$, we find that it is reduced by $\sim$ 20–25 %, while experimentally the magnetization follows a Brillouin-like function, and consequently, the experimentally observed reduction of the magnetization is only a few percent.[36] This discrepancy is due to the neglect of the quantization of the elementary excitations that follows from using a classical spin model to describe the interaction of the local magnetic moments. In the case of classical spin Hamiltonians, the low-temperature excitations consist of small-angle fluctuations of the local moments away from the mag-

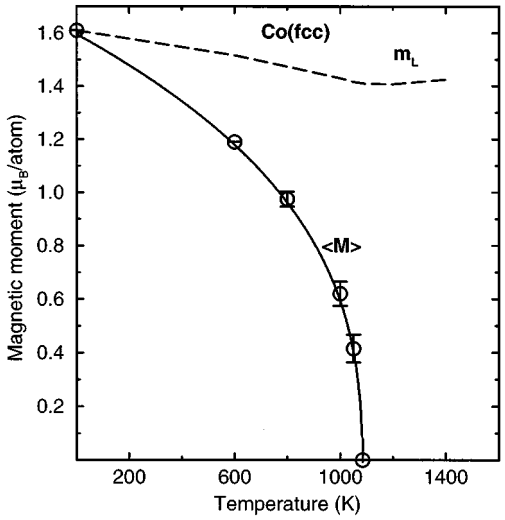

FIG. 7. The magnetization (full line), and the local magnetic moment (dashed line) of fcc Co as a function of temperature.

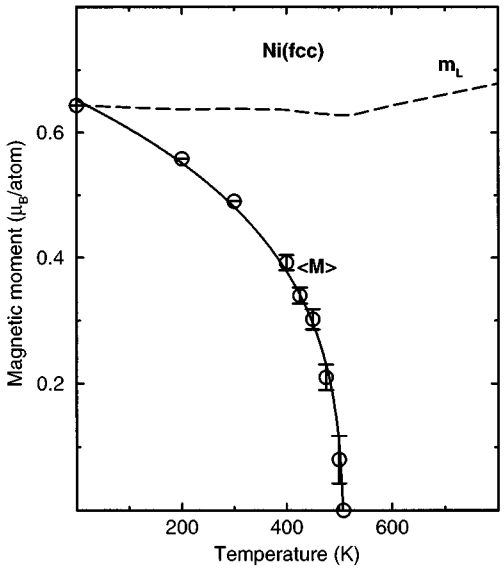

FIG. 8. The magnetization (full line), and the local magnetic moment(dashed line) of fcc Ni as a function of temperature.

netization direction. This results in a linear decrease of the magnetization as the temperature approaches zero, and as a result the calculated magnetization does not follow Bloch's $T^{3/2}$ law at low temperature. However, here we will focus on the magnetic behavior in the vicinity of the Curie temperature, and in the paramagnetic regime. We note that the classical nearest-neighbor Heisenberg Hamiltonian has an exponent of $\beta=0.36$ (Ref. 35) for the temperature dependence of the magnetization in the critical region $M\propto(T_c-T)^{\beta}$. This exponent agrees well with the experimental critical exponents which are 0.38 for Fe and Ni, and 0.42 for Co.[31] Since, as Fig. 1 shows, the nearest-neighbor Heisenberg term is the dominating contribution to the exchange interaction in our model, we expect that the critical exponents are realistic, although the estimation of the static critical exponents including the effect of the higher-order terms, i.e., the biquadratic, and bicubic terms, and the effect of fluctuations in the size of the local moment has not been performed.

B. The local magnetic moments

The average local magnetic moments as a function of temperature are shown in Fig. 6 for bcc Fe, in Fig. 7 for fcc Co, and in Fig. 8 for fcc Ni. For temperatures below the Curie temperature, the average local magnetic moment of Fe and Ni are close to their zero-temperature magnetization. For bcc Fe, the local magnetic moment increases linearly through the critical region from $2.25\mu_B$ at 0 K to $2.35\mu_B$ at 1600 K. In contrast, the local magnetic moment of Co drops from $1.63\mu_B$ to $\sim 1.4\mu_B$ at T_C. In the paramagnetic region, however, the local moment increases. The local moment of Ni shows a behavior similar to that of Co above the Curie temperature but remains constant below T_C. These results should be correlated with the calculated average angle between nearest-neighbor local moments α_{NN} which is given in Table II. We see that this angle is $\sim 75°$ which should be compared to an average angle of 90° for randomly distributed local moments. This means that the magnetic short-range order is moderate compared to what one expects from the energy only arguments outlined above when we discussed the disordered local moment state. For fcc Ni, for instance, magnetic configurations which result in a nearest-neighbor angle of 75° is not stable compared to the nonmagnetic state. For bcc Fe, the loss of magnetic energy at the

TABLE II. Magnetic properties at the theoretical Curie temperature. Here m_{loc} is the average local magnetic moment, $\sqrt{(\Delta m_{\mathrm{loc}})^2}$ is the rms fluctuation of the local magnetic moment, and α_{NN} is the average angle between nearest-neighbor magnetic moments. All three values are obtained from Monte Carlo simulations. T_C is the Curie temperature. Calculated results are presented using mean-field theory (MF), and Monte Carlo simulations (MC). Comparison is made to previous first-principles calculations, and experiment (Expt.).

System	m_{loc} (μ_B/atom)	$\sqrt{(\Delta m_{\mathrm{loc}})^2}$	α_{NN}	T_C (K)				
	Calc.	Calc.	Calc.	MF	MC	SG[a]	UK[b]	Exp.[c]
Fe bcc	2.33	0.45	74	1460	1060	1015	1095	1043
Co fcc	1.41	0.41	75	1770	1080		1012	1388
Ni fcc	0.63	0.22	75	660	510	450	412	633

[a]Reference 6.
[b]Reference 7.
[c]Reference 31.

calculated Curie temperature is ~1850 K, and this constitutes almost half of the total magnetic energy of the ferromagnetic state. Yet in the simulations, we observe the combination of sizeable average local magnetic moments, and small magnetic short-range order. This stresses the importance of spin fluctuations. It is the entropy of spin fluctuations that stabilizes the local magnetic moments. We may realize this by noting that the entropy contribution is proportional to the phase space volume δV which is thermally populated. The available phase space volume can roughly be taken to depend on the nearest-neighbor angle α_{NN}, and the local magnetic moment m_{loc} as

$$\delta V \propto \sin\alpha_{\mathrm{NN}} \delta\alpha_{\mathrm{NN}} m_{\mathrm{loc}}^2 \delta m_{\mathrm{loc}}, \tag{11}$$

where δm_{loc}, and $\delta\alpha_{\mathrm{NN}}$ is a measure of the fluctuations of the local magnetic moment and the fluctuations of the magnetic short-range order, respectively. As a result, we see that the entropy of spin fluctuations favors a sizeable local magnetic moment. This simple analysis suggests that although the local moments are not energetically favored, as it is the case in the absence of strong magnetic short-range order, sizeable local magnetic moments can nevertheless be present because the available phase space volume depends quadratically on the size of the local moment. This is in accordance with the MC simulations. At the same time, it is clear that fluctuations in the sizes of the local magnetic moments will be present, and are required to stabilize these. As it can be seen from the rms value of the fluctuation of the local magnetic moment which is given in Table II, sizeable fluctuations are in fact observed in the MC simulations. As a result of the strong effect of spin fluctuations, we get similar behavior of bcc Fe, fcc Co, and fcc Ni despite their difference in itinerant character as discussed in the previous section. The qualitative similarity of our calculated finite-temperature properties for the itinerant ferromagnets bcc Fe, fcc Co, and fcc Ni agrees well with the observation from neutron-scattering experiments[37,38] that the paramagnetic scattering of bcc Fe and fcc Ni can be described by the same scattering function. Below we present calculations of the magnetic correlations in the paramagnetic state and show that the calculated inverse correlation lengths agree well with observation.

C. The Curie temperature

The MC results for the Curie temperatures are summarized in Table II. Also given in the table are the results of previous first-principles calculations, and for comparison the observed Curie temperatures. The calculated T_C of bcc Fe agrees rather well with the observed value while the calculated values for fcc Co and fcc Ni are underestimated by ~20–25 %. It is also noteworthy that despite their differences, the three first-principles approaches result in almost the same values for T_C. Table II also contains the simplest possible estimate of the Curie temperature, i.e., that which results from a mean-field calculation assuming local moments of temperature-independent size. In this calculation we have employed the exchange constants for a local moment equal to the FM equilibrium magnetization per atom at zero temperature. The mean-field expression for the Heisenberg model reads

$$T_c^{\mathrm{MF}} = \frac{1}{3}\sum_j J_{0j}. \tag{12}$$

To facilitate the mean-field calculation, we adopted the Heisenberg model for the interatomic exchange, and fitted exchange constants for the first three neighbor shells to the spiral states. The result of this estimate is given in Table II. As it may be seen from the results, the mean-field Curie temperature is overestimated compared to the experimental numbers for Fe and Co. For Ni, the mean-field T_C has almost the same value as the observed T_C. Since it is well known that the mean-field approximation leads to a systematic overestimation of critical temperatures, one might suspect that the critical temperatures calculated from Monte Carlo simulations would result in good agreement for Fe and Co, while Ni would be underestimated. As it can be seen from Table II, these conclusions hold for Fe and Ni, while for Co the Monte Carlo simulations result in a Curie temperature which is somewhat lower than experimentally observed. As it may also be realized from Table II, at T_C the local moments of Fe and Ni fluctuate around a value close to their 0 K magnetization, while the local moment of Co is reduced from 1.63 to ~1.4. If we calculate the mean-field estimate of the Curie temperature of fcc Co using exchange constants for a local moment of 1.4, we get a mean-field T_C of 1390 K which is ~30% larger than the MC result. This is similar to the mean-field overestimation of the Curie temperature which result for Fe and Ni where the average local magnetic moment at T_C coincides with the equilibrium magnetization per atom at zero temperature.

D. The paramagnetic state

In a second set of simulations at temperatures above the Curie temperature, we calculated the static paramagnetic susceptibility χ^0 for $\overline{q}=\overline{0}$, and the real-space static magnetic correlation function $\langle \overline{m_0}\cdot\overline{m_i}\rangle$. Experimentally, the temperature dependence of the susceptibility χ^0 obeys a Curie-Weiss law, and we have investigated the calculated χ^0 and find that within the statistical errors arising from the MC simulations, the observed Curie-Weiss behavior is obeyed by the model. From the temperature dependence of the uniform susceptibility χ^0, we also determine the value of the Curie-Weiss constant. The real space static magnetic correlation function was investigated to determine the paramagnetic scattering behavior. We have derived inverse correlation lengths from the calculated correlation functions and compare to experimental values.

One can, in principle, calculate the static uniform susceptibility χ^0 from the variance of the magnetization, and as noted in the previous section, calculated this way the peak of χ^0 as a function of temperature gives a good estimate of the Curie temperature. However, using MC to calculate the absolute value of the susceptibility χ^0 from the variance of the magnetization is difficult, and requires long MC runs, and subsequent finite-size scaling. It is easier, and more accurate to calculate χ^0 directly from the definition $\chi^0 = dM/dH$ where H denotes a uniform magnetic field, and M the mag-

TABLE III. Properties of the paramagnetic state, both results of this work, previous first-principles results, and experiment (Expt.). C is the Curie-Weiss constant of the paramagnetic susceptibility. κ is the inverse correlation length derived from the pair-correlation function calculated at the temperature $T=1.25T_C$.

System	C (μ_B^2)			κ (Å^{-1})		
	This work	SG[a]	Expt.[b]	This work	SG[a]	Expt.
Fe bcc	3.0	1.28	3.41	0.38	0.37	0.40[c]
Co fcc	1.1		3.31	0.34		
Ni fcc	0.22	0.49	0.86	0.28	0.28	0.24[d]

[a]Reference 6.
[b]Reference 40.
[c]Reference 37.
[d]Reference 38.

netization. In practice, we perform a calculation with a Zeeman term from a magnetic field added to the magnetic energy. Provided the magnetic field is small enough that the response is linear, we can determine χ^0 directly from the magnetization obtained in the direction of the magnetic field. For each of the three ferromagnets, we have performed calculations for three different values of the field to ensure that we sample the linear regime of small fields. The value of the field is of the order 0.1 mRy/$\mu_B \sim 20$ T which is an order of magnitude higher than laboratory field strengths. This relative large value of the field is required to ensure that the response is significant relative to the magnetization fluctuations which result from the relative small number of sites used in the simulations. We also tested the size dependence and conclude that the main effect of increasing the number of sites is to reduce the statistical error.

As already mentioned, within the statistical errors, the calculated χ^0 obeys a Curie-Weiss law. The calculated values of the Curie-Weiss (CW) constants of bcc Fe, fcc Co, and fcc Ni are given in Table III. Also given in the table (labeled SG) are the calculated values of Staunton and Györffy,[6] and the observed values. As for the Curie temperature, the CW constant of bcc Fe is reproduced rather well. For fcc Co and fcc Ni, the CW constants are underestimated. This is in contrast to the results of Staunton and Györffy who obtained an underestimate of the CW constants of both bcc Fe and fcc Ni. The absolute value of the CW constant of fcc Ni calculated by Staunton and Györffy does however agree considerably better with observation than the value calculated in the present work.

The real-space static magnetic correlation function $\langle \overline{m_0} \cdot \overline{m_i} \rangle$ has been calculated from simulations on 2744 (14^3) sites. From general arguments,[34] the paramagnetic real-space correlation function is expected to show only a weak dependence on the size of the computational box. The resulting real-space correlations of bcc Fe at two temperatures in the paramagnetic regime are shown in Fig. 9. In the figure, we also show the result of fitting a simple Ornstein-Zernike correlation function $\propto \exp(-\kappa d)/d$ to the calculated real-space correlations. In this expression, κ is the inverse correlation length, and d is the intersite distance. In the fitting, we have neglected the nearest, and next-nearest neighbor correlation as the simple Ornstein-Zernike correlation function is expected to hold in the long-wavelength limit. As

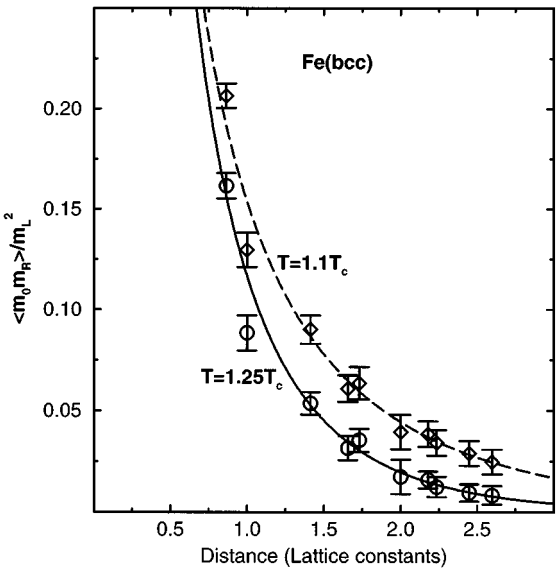

FIG. 9. The real-space static magnetic correlation function of bcc Fe at the temperatures $1.1T_C$ (diamonds), and $1.25T_C$ (circles). Lines are the fit to the Ornstein-Zernike expression.

can be seen in Fig. 9, the calculated correlations show some oscillations which is not contained in the monotoneous decrease of the Ornstein-Zernike function. The oscillations which are common for the two temperatures are rather small compared to the statistical uncertainty of the correlations. The inverse correlation lengths that can be derived from the assumption of the Ornstein-Zernike correlation function are 0.19 and 0.38 Å^{-1} for temperatures of $1.10T_C$, and $1.25T_C$, respectively. These values corresponds to a value $\eta=0.75$ for the critical exponent of the correlation length. Given the rather large uncertainty in the determination of κ especially for $T=1.10T_C$, this value of η compares favourably to the observed value of $\eta=0.70$.[31] In Table III, we give the calculated values of the inverse correlation length κ for the temperature $1.25T_C$ for the three systems considered in the present study. To facilitate a comparison to the experimental values which are also given in the table, we kept the ratio of paramagnetic temperature to the Curie temperature the same in calculation, and experiment. As it can be seen, calculation agrees rather well with experiment for both bcc Fe and fcc Ni. We were not able to find experimental values of κ for fcc Co. The uncertainty in the determination of κ was estimated to be $\sim$ 0.03 Å^{-1} for bcc Fe and $\sim$ 0.02 Å^{-1} for fcc Ni. These numbers are comparable to the deviation from observation. Even better agreement is obtained between the present calculation, and the calculation of Staunton and Györffy. The close agreement is somewhat surprising since the approach of Staunton and Györffy is very different from that of the present work. It should be noted that the different inverse correlation lengths obtained for bcc Fe, fcc Co, and fcc Ni are closely related to their different lattice constants. In units of inverse lattice constants, κ of bcc Fe is 1.05, κ of fcc Co is 1.19, and κ of fcc Ni is 0.97. That is, the extent of the correlations is about the same measured in lattice units. In contrast, the absolute value of the static correlations differ, as can be realized from their different uniform susceptibilities χ^0.

As witnessed by the nearest-neighbor spin angle α_{NN} given in Table II, the present treatment results in a relatively small amount of magnetic short-range order. This is in contrast to some of the early theoretical work[1,18] which, based on the experiments of Mook *et al.*[41] and Lynn,[42] required considerable magnetic short-range order. Since then the analysis of Edwards,[43] and neutron-scattering experiments at Brookhaven[38,39,44] have clarified the observations made in the early experiments. While we cannot rule out the existence of strong magnetic short-range order, it is clear from the present work, as well as from the work of Staunton and Györffy[6] that a paramagnetic state containing only small magnetic short-range order can explain the paramagnetic scattering observed experimentally.

V. CONCLUSIONS

We have presented a magnetic energy functional which is based on the set of local magnetic moments $\{\overline{m_i}\}$ and describes the magnetic energy of an arbitrary magnetic configuration. The ordering of the local magnetic moments is described by a generalized Heisenberg Hamiltonian in which the direction of the local moments are represented as classical vectors. First of all, the exchange interactions depend on the size of the local magnetic moments. In addition, an on-site exchange contribution is derived from fixed spin moment calculations for the constrained ferromagnetic states. The sum of on-site and local exchange energy provides a magnetic energy functional which includes the correlation between the stability of the local magnetic moment, and the ordering of the local moments. We have presented self-consistent LMTO calculations of zero-temperature magnetic properties within the local-spin-density approximation to the density-functional formalism. Calculations have been performed for bcc Fe, fcc Co, and fcc Ni both for the constrained ferromagnetic states, and for a number of spin spiral states using the fixed spin moment technique. The zero-temperature results of these calculations compare well with the experimentally observed low-temperature properties, although we note that some discrepancy was found for the spin-wave stiffness constants of bcc Fe and fcc Ni.

The results of the self-consistent electronic-structure calculations were subsequently used to calculate the parameters of our magnetic energy functional. In a subsequent set of Monte Carlo simulations, we applied the model magnetic energy functional to determine the equilibrium magnetic properties of the itinerant ferromagnets Fe, Co, and Ni. In the simulations, we allowed all degrees of freedom to vary. For our chosen description of the magnetic configurations, they include both size, and direction of the local magnetic moments on each site. From the MC simulations, we determined finite-temperature magnetic properties such as the magnetization curve, the Curie temperature, and the behavior of the local magnetic moment as a function of temperature. The calculated magnetization curve was found to deviate considerably from the observed magnetization curve. We believe this is a consequence of the separation of quantum-mechanical and statistical mechanical averages which results from our mapping to a Hamiltonian that describes the local magnetic moments classically, and include quantum effects only in the calculation of the exchange constants. Our calculated Curie temperature of bcc Fe agrees very well with the experimental Curie temperature, while the Curie temperatures of fcc Co and fcc Ni are underestimated by about 20-25%. The calculated Curie temperatures agree very well with previous first-principles calculations of Staunton and Györffy[6] and Uhl and Kübler.[7]

We also investigated the paramagnetic state of the $3d$ ferromagnets. We presented calculations of the uniform paramagnetic susceptibility χ^0 and the inverse correlation lengths derived from the static magnetic correlation function. Within the statistical uncertainty of the MC simulations, we found that the uniform paramagnetic susceptibility χ^0 obeys a Curie-Weiss behavior, and we determined the Curie-Weiss (CW)constants of the $3d$ ferromagnets. As for the Curie temperature, the CW constant of bcc Fe agrees very well with experiment. This is in contrast to the previous work of Staunton and Györffy.[6] For fcc Co and fcc Ni, however we calculate a CW constant which is only a fraction of the experimentally observed CW constant whereas Staunton and Györffy get reasonable agreement with experiment for fcc Ni. It should be noted, that the CW constant of fcc Ni is only 1/4'th of the CW constant of bcc Fe, and as a consequence an absolute error which is acceptable for bcc Fe can for fcc Ni be of the order of the CW constant itself. We found that the static magnetic correlation functions fit well to the paramagnetic scattering behavior observed experimentally. The calculated inverse correlation lengths are in good agreement with experimental values obtained from neutron-scattering experiments.

Further improvements are certainly possible. The effect of including self-consistent calculations for other constrained magnetic structures than the spin spirals would be of interest, and could clarify the size of multisite interactions which have been neglected in the present work. We have completely neglected the effect of Stoner excitations. However, due to the large Stoner-Curie temperatures obtained in the local-spin-density approximation (LSDA), we expect the effect of these excitations to be small. The effect of the LSDA itself would also be of interest, as would an investigation of the approximation in the self-consistent calculations of using a single spin quantization for each site. Other effects such as thermal expansion, and lattice vibrations are more difficult to handle at present but may obviously influence the magnetic properties. In a wider perspective, mapping to a quantum-mechanical representation of the magnetic state instead of the classical representation used in the present work would be very interesting, and could improve the description of the magnetic properties, especially below T_C.

In summary, a model based on a coarse-grained description of the magnetic state in terms of site-dependent local magnetic moments was used to calculate the magnetic energy. The derived magnetic energy expression was shown to account for most of the qualitative features of the itinerant ferromagnetism in bcc Fe, fcc Co, and fcc Ni. The simple division of the magnetic energy into on-site and local intersite exchange contributions provides a simple picture of the itinerant ferromagnets. Hence, we were able to characterize bcc Fe as a weak itinerant ferromagnet whereas the ferromagnetism of fcc Co, and in particular of fcc Ni was found

to have a strong itinerant character. Despite the difference in itinerancy, the finite-temperature properties of all three systems are closely related. This was shown to be a consequence of the entropy of spin fluctuations. Spin fluctuations stabilizes the local magnetic moments at finite-temperatures and this leads to similar finite temperature behavior of bcc Fe, fcc Co, and fcc Ni. The dominating role of spin fluctuations leads to a paramagnetic state consisting of sizeable local moments in a weak short-range ordered state.

ACKNOWLEDGMENTS

We thank Dr. I. A. Abrikosov (Uppsala University), and Dr. H. L. Skriver (The Technical University of Denmark) for many enlightening discussions, and valuable comments. N.M.R. would like to thank the EU for financial support through Contract No. ERBCHRXCT 940630, under the network for *X-ray Studies of the Structural and Electronic Properties of Magnetic Materials*.

[1] M. V. You, V. Heine, A. J. Holden, and P. J. Lin-Chung, Phys. Rev. Lett. **44**, 1282 (1980).
[2] T. Oguchi, K. Terakura, and N. Hamada, J. Phys. F **13**, 145 (1983).
[3] A. J. Pindor, J. Staunton, G. M. Stocks, and H. Winter, J. Phys. F **13**, 979 (1983).
[4] A. I. Liechtenstein, M. I. Katsnelson, V. P. Antropov, and V. A. Gubanov, J. Magn. Magn. Mater. **67**, 65 (1987).
[5] M. U. Luchini and V. Heine, J. Phys. C **1**, 8961 (1989).
[6] J. B. Staunton and B. L. Györffy, Phys. Rev. Lett. **69**, 371 (1992).
[7] M. Uhl and J. Kübler, Phys. Rev. Lett. **77**, 334 (1996).
[8] V. P. Antropov, M. I. Katsnelson, M. van Schilfgaarde, and B. N. Harmon, Phys. Rev. Lett. **75**, 729 (1995).
[9] V. P. Antropov, M. I. Katsnelson, B. N. Harmon, M. van Schilfgaarde, and D. Kusnezov, Phys. Rev. B **54**, 1019 (1996).
[10] L. M. Sandratskii and P. G. Guletskii, J. Phys. F **16**, 43 (1986).
[11] J. Kübler, K.-H. Höck, J. Sticht, and A. R. Williams, J. Phys. F **18**, 469 (1988).
[12] M. Uhl, L. M. Sandratskii, and J. Kübler, Phys. Rev. B **50**, 291 (1994).
[13] T. Oguchi, K. Terakura, and A. R. Williams, Phys. Rev. B **28**, 6443 (1983).
[14] T. Moriya, J. Phys. Soc. Jpn. **40**, 933 (1976).
[15] D. M. Edwards, J. Phys. F **6**, L289 (1976).
[16] J. Hubbard, Phys. Rev. B **19**, 2626 (1979).
[17] H. Hasegawa, J. Phys. Soc. Jpn. **46**, 1504 (1979).
[18] V. Korenman, J. L. Murray, and R. E. Prange, Phys. Rev. B **16**, 4032 (1977).
[19] P. Mohn and E. P. Wohlfarth, J. Phys. F **17**, 2421 (1987).
[20] V. L. Moruzzi, P. M. Marcus, K. Schwarz, and P. Mohn, Phys. Rev. B **34**, 1784 (1986).
[21] A. R. Mackintosh and O. K. Andersen, in *Electrons at the Fermi Surface*, edited by M. Springford (Cambridge University Press, Cambridge, 1980), p. 149.
[22] O. K. Andersen, Z. Pawlowska, and O. Jepsen, Phys. Rev. B **34**, 5253 (1986).
[23] O. K. Andersen, J. Madsen, U. K. Poulsen, O. Jepsen, and J. Kollar, Physica B **86-88**, 247 (1977).
[24] S. H. Vosko, L. Wilk, and M. Nusair, Can J. Phys. **58**, 1200 (1980).
[25] O. K. Andersen, Phys. Rev. B **12**, 3060 (1975).
[26] H. L. Skriver, *The LMTO Method* (Springer-Verlag, Berlin, 1984).
[27] O. K. Andersen and O. Jepsen, Phys. Rev. Lett. **53**, 2571 (1984).
[28] H. Danan, A. Herr, and A. J. P. Meyer, J. Appl. Phys. **39**, 669 (1968).
[29] H. P. Myers, and W. Sucksmith, Proc. R. Soc. London Ser. A **207**, 427 (1951).
[30] M. W. Stringfellow, J. Phys. C **1**, 950 (1968).
[31] E. P. Wohlfarth, in *Ferromagnetic Materials*, edited by E. P. Wohlfarth (North-Holland, Amsterdam, 1980), p. 1.
[32] P. Mitchell, and D. McPaul, Phys. Rev. B **32**, 3272 (1985).
[33] N. Metropolis, A. W. Rosenbluth, M. N. Rosenbluth, A. H. Teller, and E. Teller, J. Chem. Phys. **21**, 1087 (1953).
[34] K. Binder, in *Monte Carlo Methods in Statistical Physics*, edited by K. Binder (Springer, New York, 1979).
[35] R. L. Stephenson and P. J. Wood, Phys. Rev. **173**, 475 (1968).
[36] J. Crangle, *The Magnetic Properties of Solids* (Edward Arnold, London, 1977).
[37] G. Shirane, P. Böni, and J. P Wicksted, Phys. Rev. B **33**, 1881 (1986).
[38] O. Steinsvoll, C. F. Majkrzak, G. Shirane, and J. P. Wicksted, Phys. Rev. B **30**, 2377 (1984).
[39] J. P. Wicksted, G. Shirane, and O. Steinsvoll, Phys. Rev. B **29**, 488 (1984).
[40] W. Sucksmith and R. R. Pearce, Proc. R. Soc. London Ser. A **167**, 189 (1938).
[41] H. A. Mook, J. W. Lynn, and R. M. Nicklow, Phys. Rev. Lett. **30**, 556 (1973).
[42] J. W. Lynn, Phys. Rev. B **11**, 2624 (1975).
[43] D. M. Edwards, J. Magn. Magn. Mater. **36**, 213 (1983).
[44] Y. J. Uemura, G Shirane, O. Steinsvoll, and J. Wicksted, Phys. Rev. Lett. **51**, 2322 (1983).